

Temperature-Responsive Protein Pores

Yuni Jung,^{†,‡} Hagan Bayley,[§] and Liviu Movileanu^{*,||}

Contribution from the Department of Medical Biochemistry and Genetics, The Texas A&M University System Health Science Center, College Station, Texas 77843-1114, Chemistry Research Laboratory, Department of Chemistry, Oxford University, Mansfield Road, Oxford OX1 3TA, United Kingdom, Department of Physics, Syracuse University, 201 Physics Building, Syracuse, New York 13244-1130, and Structural Biology, Biochemistry, and Biophysics Program, Syracuse University, 111 College Place, Syracuse, New York 13244-4100

Received August 10, 2006; E-mail: lmovilea@physics.syr.edu

Abstract: We describe temperature-responsive protein pores containing single elastin-like polypeptide (ELP) loops. The ELP loops were placed within the cavity of the lumen of the α -hemolysin (α HL) pore, a heptamer of known crystal structure. The cavity is roughly spherical with a molecular surface volume of about 39 500 Å³. In an applied potential, the wild-type α HL pore remained open for long periods. In contrast, the ELP loop-containing α HL pores exhibited transient current blockades, the nature of which depended on the length and sequence of the inserted loop. Together with similar results obtained with poly(ethylene glycols) covalently attached within the cavity, the data suggest that the transient current blockades are caused by excursions of ELP into the transmembrane β -barrel domain of the pore. Below its transition temperature, the ELP loop is fully expanded and blocks the pore completely, but reversibly. Above its transition temperature, the ELP is dehydrated and the structure collapses, enabling a substantial flow of ions. Potential applications of temperature-responsive protein pores in medical biotechnology are discussed.

Introduction

With the inspiration of examples from nature, a variety of polymeric materials have been designed that respond to external physical and chemical stimuli such as temperature, pH, electric fields, light, ionic strength, and various chemicals.^{1–4} For example, the elastin-like polypeptides (ELPs) undergo a sharp inverse temperature transition and become more ordered as the temperature increases.^{5–15} Below its transition temperature T_i ,

an ELP is soluble in water, but as the temperature is raised above T_i , it aggregates. This inverse temperature transition has been attributed to the hydrophobic collapse of individual ELP molecules with the expulsion of waters that contact the hydrophobic side chains of the polypeptide in the expanded form.

Here, we describe temperature-responsive pores containing a single ELP loop. The ELP loop is engineered within the cavity that forms part of the lumen of the staphylococcal α -hemolysin (α HL) pore, a mushroom-shaped heptameric protein of known structure (Figure 1A).¹⁶ The cavity measures ~ 45 Å in diameter, and its molecular surface volume is $\sim 39\,500$ Å³, as determined from the X-ray crystal structure of the pore.¹⁶ Recently, tandem repeats of a Gly/Ser-containing sequence have been placed in the cavity.¹⁷ When α HL pores were assembled into heteroheptamers comprising wild-type subunits and Gly/Ser-loop-containing subunits, up to 175 exogenous residues were accommodated within the cavity of the pore.

In this work, we show a dramatic change in the functional properties of the α HL pore when the engineered ELP loop acts as a temperature-responsive gating mechanism. In an applied transmembrane potential, the wild-type α HL pore maintains its open state for long periods.^{18,19} In contrast, the ELP loop-containing α HL pore exhibits an open state decorated by

[†] The Texas A&M University System Health Science Center.

[‡] Present address: Cardiovascular Research Institute, University of California at San Francisco, San Francisco, CA 94143-2532.

[§] Oxford University.

^{||} Syracuse University.

- (1) Galaev, I. Y.; Mattiasson, B. *Trends Biotechnol.* **1999**, *17*, 335–340.
- (2) Ding, Z. L.; Fong, R. B.; Long, C. J.; Stayton, P. S.; Hoffman, A. S. *Nature* **2001**, *411*, 59–62.
- (3) Jeong, B.; Gutowska, A. *Trends Biotechnol.* **2002**, *20*, 305–311.
- (4) Russell, T. P. *Science* **2002**, *297*, 964–967.
- (5) Luan, C. H.; Parker, T. M.; Prasad, K. U.; Urry, D. W. *Biopolymers* **1991**, *31*, 465–475.
- (6) Urry, D. W.; Gowda, D. C.; Parker, T. M.; Luan, C. H.; Reid, M. C.; Harris, C. M.; Pattanaik, A.; Harris, R. D. *Biopolymers* **1992**, *32*, 1243–1250.
- (7) Urry, D. W. *Angew. Chem., Int. Ed. Engl.* **1993**, *32*, 819–841.
- (8) Urry, D. W. *J. Phys. Chem. B* **1997**, *101*, 11007–11028.
- (9) Reiersen, H.; Clarke, A. R.; Rees, A. R. *J. Mol. Biol.* **1998**, *283*, 255–264.
- (10) Urry, D. W.; Hugel, T.; Seitz, M.; Gaub, H. E.; Sheiba, L.; Dea, J.; Xu, J.; Parker, T. *Philos. Trans. R. Soc. London, B: Biol. Sci.* **2002**, *357*, 169–184.
- (11) Hyun, J.; Lee, W. K.; Nath, N.; Chilkoti, A.; Zauscher, S. *J. Am. Chem. Soc.* **2004**, *126*, 7330–7335.
- (12) Nicolini, C.; Ravindra, R.; Ludolph, B.; Winter, R. *Biophys. J.* **2004**, *86*, 1385–1392.
- (13) Meyer, D. E.; Chilkoti, A. *Biomacromolecules* **2004**, *5*, 846–851.
- (14) Schreiner, E.; Nicolini, C.; Ludolph, B.; Ravindra, R.; Otte, N.; Kohlmeyer, A.; Rousseau, R.; Winter, R.; Marx, D. *Phys. Rev. Lett.* **2004**, *92*.
- (15) Baer, M.; Schreiner, E.; Kohlmeyer, A.; Rousseau, R.; Marx, D. *J. Phys. Chem. B* **2006**, *110*, 3576–3587.

(16) Song, L. Z.; Hobaugh, M. R.; Shustak, C.; Cheley, S.; Bayley, H.; Gouaux, J. E. *Science* **1996**, *274*, 1859–1866.

(17) Jung, Y. H.; Cheley, S.; Braha, O.; Bayley, H. *Biochemistry* **2005**, *44*, 8919–8929.

(18) Movileanu, L.; Cheley, S.; Bayley, H. *Biophys. J.* **2003**, *85*, 897–910.

(19) Movileanu, L.; Schmittschmitt, J. P.; Scholtz, J. M.; Bayley, H. *Biophys. J.* **2005**, *89*, 1030–1045.

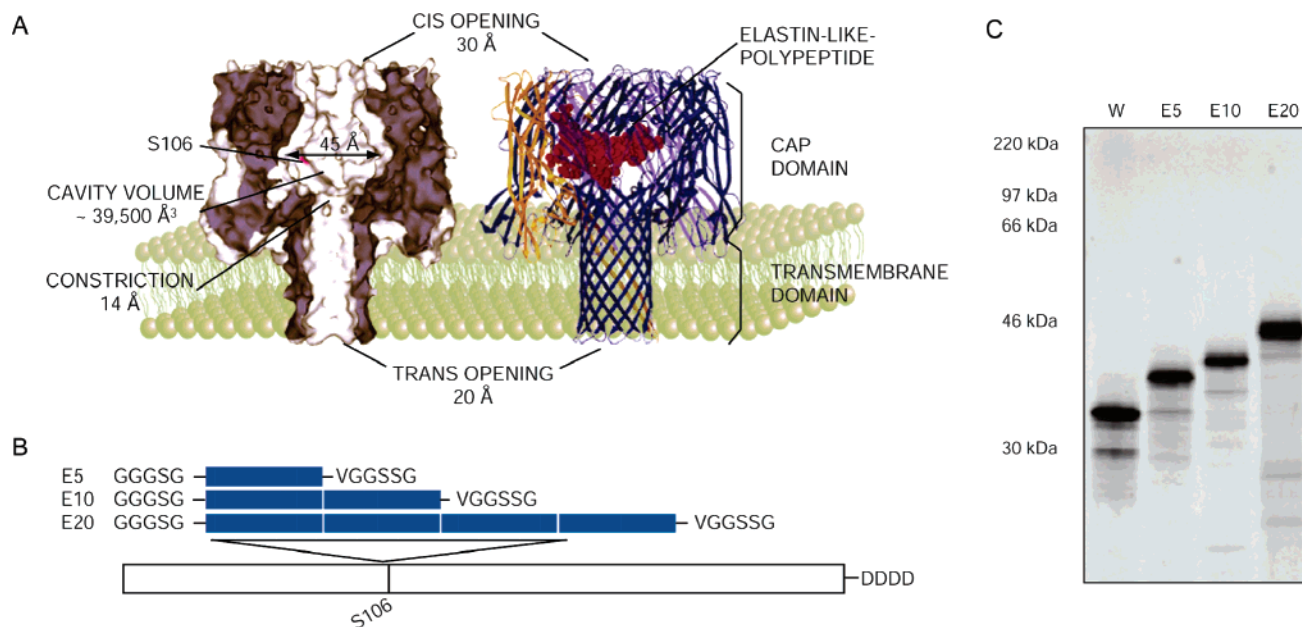


Figure 1. Elastin-like polypeptide-containing α HL. (A) Three-dimensional models of the wild-type α -hemolysin (α HL, W₇) pore and the elastin-like polypeptide- (ELP-) containing α HL pore. One of the seven Ser residues at position 106, which corresponds to the ELP insertion site, is shown in violet. A model of the ELP loop-containing α HL subunit (here, the E10 subunit), generated by Swiss-Model,²⁸ replaced one of the wild-type subunits (W). The ELP loop is shown as a space-filling representation (maroon). The E10 subunit (yellow) and six wild-type (W) subunits (blue) are shown as ribbon diagrams. (B) Four aspartate residues (D4) were placed on the C terminus of α HL to facilitate the separation of various heteroheptamers.²³ Concatemered ELP repeats with flanking Gly-Ser linkers were inserted between positions 105 and 106 of the W subunit. The subunits containing an ELP insert were denoted by E(*n*), where *n* represents the total number of inserted VPGGG repeats (5, 10, or 20). Each blue box represents five repeats of VPGGG sequences. The W subunit is shown as a white box. (C) Autoradiogram of a 10% SDS polyacrylamide gel showing the monomeric subunits E5, E10, and E20 and the W subunit.

transient current blockades. Below its transition temperature T_i , the ELP loop is in an expanded conformation^{7,8,10,20,21} and produces full current blockades. Above its transition temperature T_i , the ELP loop is dehydrated due to the hydrophobic collapse^{7–15,22} and causes partial current blockades. We demonstrate that the features of both the transient ELP-induced current blockades and the open-state currents are dependent on the peptide length as well as its sequence.

With further development, we anticipate that such an engineered α HL pore with a built-in temperature-responsive gating mechanism will be useful in biotechnological applications. For example, temperature-responsive protein pores might be used in drug delivery, to release the contents of capsules such as liposomes, or as biotherapeutics, to permeabilize cells to cytotoxic drugs.

Experimental Methods

Generation of a Subcloning Vector. The endogenous *EarI* sites of pT7-L5-D4¹⁷ were removed by polymerase chain reaction (PCR) and in vivo recombination²³ (Supporting Information, Figure S1A). The resulting plasmids pYH1-L5-D4 were digested with *AvaI*, followed by replacement of the small fragment with the DNA cassette 5'-TCGGGGGTATGAAGAGAGCAGATGCATGGC-3' (sense) and 5'-CCGAGCCATGCATCTGCTCTCTTCATACCC-3' (antisense) to introduce an *EarI* site (underlined) in between *AvaI* sites. The resulting subcloning vectors were denoted as pYH1-EC-D4 (Supporting Information, Figure S1B). Replacements were verified by DNA sequencing.

Generation of a Subcloning Vector Encoding Monomeric ELP Repeat Unit. The plasmids containing the gene that encodes the ELP

repeat unit (pYH1-EM-D4) were generated by ligation of two double-stranded oligonucleotides formed by the single-stranded oligonucleotides, 5'-TATGAACCTCTTCCGTACCCGGAGGTGGCGTGCCAGGTGGCGGTGTCCCA-3' (EM001), 5'-GGTGGCGGAGTCCAGGTGGAGGCGTCCCTGGCGGAGGTGTATGAAGAGCTA-3' (EM002), 5'-GCCACCTGGGACACCGCCACCTGGCAGCCACCTCCGGGTACGGAAGAGTTCA-3' (EM003), and 5'-AGCTTAGCTCTTCATACACCTCCGCCAGGGACGCCTCCACCTGGAACCTCC-3' (EM004), into the pYH1-L5-D4 from which the central *NdeI*–*HindIII* fragment was removed (Supporting Information, Figure S1C). The *EarI* sites, which flank the repeat unit, are underlined. Prior to ligation, the 5' ends of EM002 and EM003 were phosphorylated by T4 polynucleotide kinase (New England BioLabs, Beverly, MA) followed by enzyme inactivation at 65 °C for 20 min. The repeat unit encoded five tandem repeats of VPGGG. The ligated product was transformed into SURE2 supercompetent *Escherichia coli* cells (Stratagene, La Jolla, CA) to prevent in vivo recombination. The replacement was verified by DNA sequencing.

Construction of α HL Genes with DNA Inserts Encoding ELP Repeats. Concatemers of the repeat unit were prepared by ligation of purified repeat units from pYH1-EM-D4 plasmid by use of *EarI* sites and an unphosphorylated “cap DNA” (1:20 molar ratio of cap/repeat unit) at 16 °C for 16 h (Supporting Information, Figure S1C).¹⁷ The cap DNA is designed to control the extent of concatemeration and to provide the 3' end *MluI* site for further cloning. The cap DNA encodes VGGSSGSIDTKEYA (5'-GTAGGAGGCTCCTCGGGTTCGATTGATACAAAAGAGTA-3' (sense) and 5'-CGCGTACTCTTTGTATCAATCGAACCCGAGGAGCCTCC-3' (antisense)). The italic-type letters indicate the exogenous residues, whereas the other letters show the endogenous L5 α HL residues (S¹¹¹IDTKEYA¹¹⁸).¹⁷ Head-to-tail ligated dimer and tetramer repeats were purified from a preparative 2.5% agarose gel by use of a Qiaex II gel extraction kit (Qiagen, Valencia, CA), followed by ligation to the large *EarI*–*MluI* fragment of pYH1-EC-D4 and transformation into SURE2 supercompetent *E. coli* cells (Stratagene, La Jolla, CA). The final constructs consisted of five residues

(20) Li, B.; Alonso, D. O. V.; Daggett, V. *J. Mol. Biol.* **2001**, *305*, 581–592.
 (21) Li, B.; Daggett, V. *Biopolymers* **2003**, *68*, 121–129.
 (22) Rousseau, R.; Schreiner, E.; Kohlmeier, A.; Marx, D. *Biophys. J.* **2004**, *86*, 1393–1407.
 (23) Howorka, S.; Bayley, H. *BioTechniques* **1998**, *25*, 764.

(GGGSG) upstream of ELPs, the ELP repeats (25, 50, or 100 residues) and six residues downstream (VGGSSG) of ELPs (Figure 1B). The flexible Gly/Ser linker sequences were placed between ELP repeats and α HL to provide minimal structural perturbation. The modified α HL genes were sequenced by Lone Star Labs Co. (Houston, TX).

Synthesis, Oligomerization, and Purification of the α HL Protein Pores. The α HL polypeptides were synthesized and oligomerized by in vitro coupled transcription and translation in the presence of purified rabbit red blood cell membranes and then purified by SDS-PAGE, as described previously.^{17,24}

Electrical Recordings in Planar Bilayers. Electrical recordings were carried out with planar bilayer lipid membranes (BLMs).^{25–27} The cis and trans chambers of the apparatus were separated by a 25- μ m thick Teflon septum (Goodfellow Corp., Malvern, PA). A 1,2-diphytanoyl-*sn*-glycerophosphocholine (Avanti Polar Lipids, Alabaster, AL) bilayer was formed across a 60- μ m wide aperture in the septum. The electrolyte in both chambers was 2 M KCl and 10 mM potassium phosphate buffer, pH 7.4. The α HL pores were introduced by adding gel-purified heteroheptamers (0.5–2.0 μ L) to the cis chamber, to give a final protein concentration of 0.05–0.3 ng/mL. Single-channel currents were recorded by using a patch clamp amplifier (Axopatch 200B, Axon Instruments, Foster City, CA) connected to Ag/AgCl electrodes through agar bridges. The cis chamber was grounded and a positive current (upward deflection) represents positive charge moving from the trans to cis side. A Pentium PC was equipped with a DigiData 1322A A/D converter (Axon) for data acquisition. The signal was low-pass-filtered with an 8-pole Bessel filter at a frequency of 20 kHz and sampled at 50 kHz. For data acquisition and analysis, we used the pClamp 9.2 software package (Axon).

Temperature Controller for Single-Channel Electrical Recordings with Planar Lipid Bilayers. The temperature-control experiments were carried out by using a Dagan HCC-100A controller (Dagan Corp., Minneapolis, MN), which was adapted to planar bilayer recordings. The HCC-100A heats and cools an aluminum thermal stage through Peltier elements. The temperature was computer-controlled through an external command connection via the Digidata 1322A (Axon). Temperature was simultaneously monitored in the aluminum stage and in the bilayer chamber with thermocouple probes.

Molecular Graphics. The ELP loop-containing subunit (E10) was generated by Swiss model.²⁸ The α HL model (7ahl) was generated with the SPOCK 6.3 software package.²⁹

Results

Preparation of an ELP Loop-Containing α HL Pore. We have generated α HL pores with a single ELP loop. These ELP loop-containing α HL pores were consisted of one ELP-containing α HL (E) subunit and six wild-type α HL (W) subunits (Figure 1A). Each E subunit was generated by placing an ELP with Gly/Ser-based linkers upstream of the 106 position of the α HL protein (Figure 1B). To examine the effect of the length of the inserted loop, we have chosen three ELPs with the sequence (VPGGG)_{*n*}, where *n* is 5, 10, or 20. The ELP loop-containing subunits were denoted as E5, E10, and E20 for the constructs with 5, 10, and 20 repeats of VPGGG, respectively (Figure 1B). If we take into consideration the Gly/Ser-based

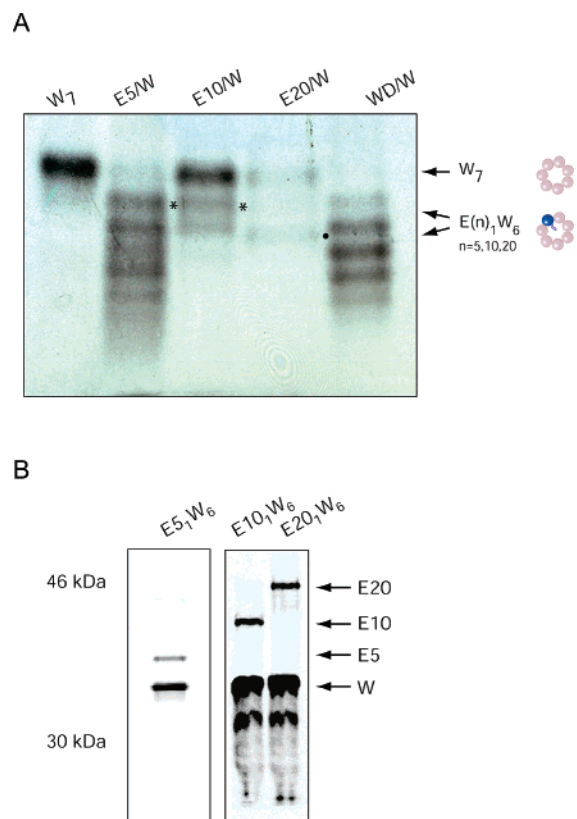


Figure 2. Heteromer preparation. (A) Autoradiogram of an SDS-5% polyacrylamide gel presenting heteroheptamers of E5/W, E10/W, and E20/W. Cartoons of the heteroheptamers with one E subunit [$E(n)_1W_6$, dotted or starred] are shown on the right side. WD is a wild-type subunit with a D4 tail placed on the C terminus. (B) Stoichiometry of purified heteroheptamers (dotted or starred) in panel A was confirmed by a second SDS-10% polyacrylamide gel after heating to dissociate them into monomers.^{17,38}

linkers, then the E5, E10, and E20 subunits contained totals of 36, 61, and 111 foreign residues, respectively. The apparent molecular masses of the E5, E10, and E20 subunits, prepared by in vitro transcription and translation (IVTT) in the presence of [³⁵S]methionine, as determined by sodium dodecyl sulfate-polyacrylamide gel electrophoresis (SDS-PAGE) (Figure 1C; 35, 37, and 45 kDa, respectively), were in accord with the calculated molecular masses (36.4, 38.2, and 41.9 kDa, respectively).

The ELP loop-containing α HL pores were prepared by IVTT in the presence of [³⁵S]methionine and purified rabbit erythrocyte membranes.^{30,31} Heteroheptamers with one ELP loop-containing subunit, E_1W_6 , were separated from other heptamers (W_7 , E_2W_5 , E_3W_4 , E_4W_3 , E_5W_2 , and E_6W_1) by SDS-PAGE (Figure 2A). The four-aspartate-residue tail (D4), which was placed on the C terminus of the E subunits (Figure 1B), allowed identification of the number of the E subunits present in each heteroheptamer by the electrophoretic shifts, as shown in previous studies.^{17,32} Heteroheptamers with E5 (or E10) and W subunits showed downward electrophoretic shifts in accordance with the number of oligoaspartate tails (Figure 2A, starred). However, the $E_{20}W_6$ proteins (Figure 2A, dotted) showed an anomalously fast electrophoretic mobility compared with the

(24) Movileanu, L.; Cheley, S.; Howorka, S.; Braha, O.; Bayley, H. *J. Gen. Physiol.* **2001**, *117*, 239–251.

(25) Movileanu, L.; Howorka, S.; Braha, O.; Bayley, H. *Nat. Biotechnol.* **2000**, *18*, 1091–1095.

(26) Movileanu, L.; Bayley, H. *Proc. Natl. Acad. Sci. U.S.A.* **2001**, *98*, 10137–10141.

(27) Montal, M.; Mueller, P. *Proc. Natl. Acad. Sci. U.S.A.* **1972**, *69*, 3561–3566.

(28) Guex, N.; Peitsch, M. C. *Electrophoresis* **1997**, *18*, 2714–2723.

(29) Christopher, J. A. *SPOCK: the structural properties observation and calculation kit*; Center for Macromolecular Design, Texas A&M University: College Station, TX, 1998.

(30) Walker, B.; Krishnasastri, M.; Zorn, L.; Kasianowicz, J. J.; Bayley, H. *J. Biol. Chem.* **1992**, *267*, 10902–10909.

(31) Cheley, S.; Braha, G.; Lu, X. F.; Conlan, S.; Bayley, H. *Protein Sci.* **1999**, *8*, 1257–1267.

(32) Howorka, S.; Cheley, S.; Bayley, H. *Nat. Biotechnol.* **2001**, *19*, 636–639.

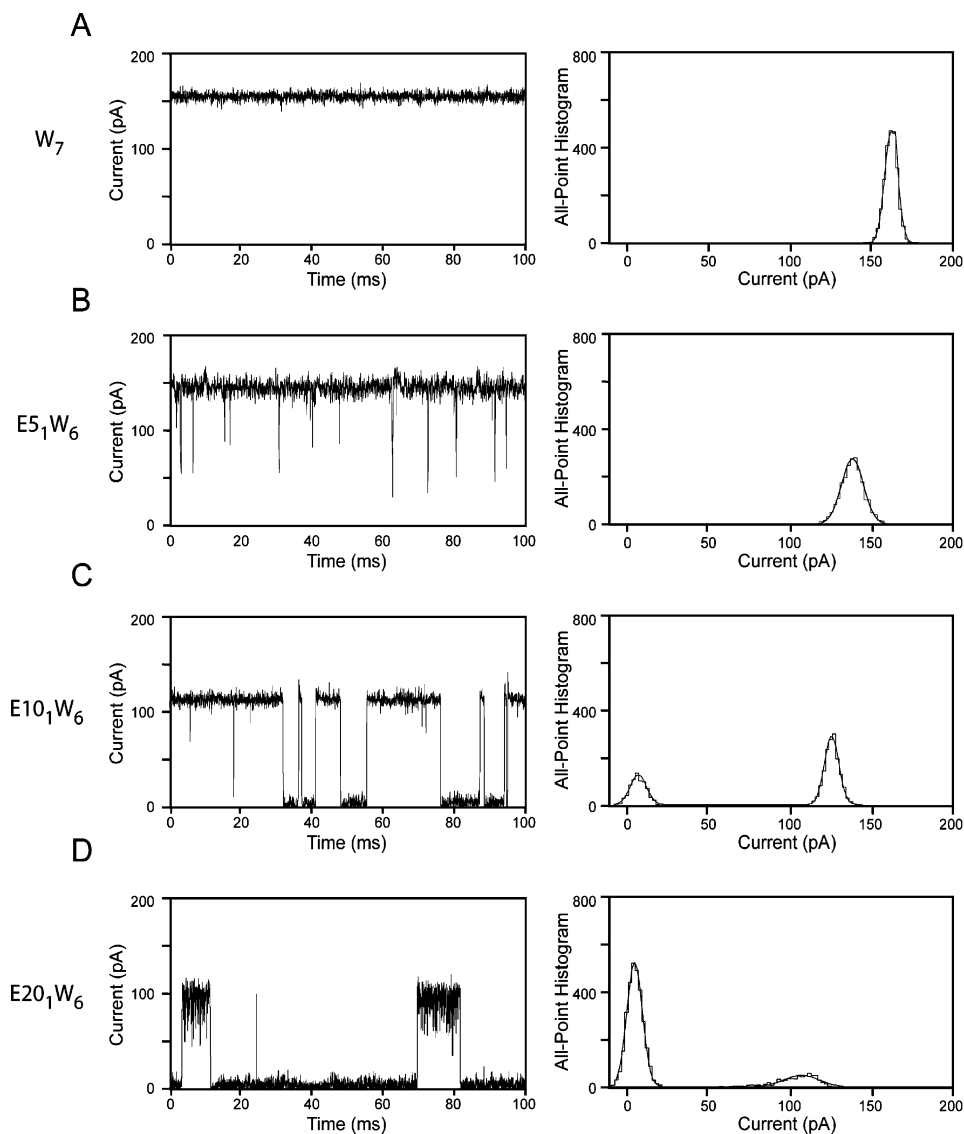


Figure 3. Representative single-channel electrical recordings of (A) WT- α HL (W_7), (B) $E5_1W_6$, (C) $E10_1W_6$, and (D) $E20_1W_6$ recorded at room temperature (23 ± 0.5 °C) in 2 M KCl and 10 mM potassium phosphate buffer, pH 7.4. The transmembrane potential was +80 mV.

WD_1W_6 proteins, where WD is a wild-type subunit with a D4 tail placed on the C terminus. To confirm the purity and stoichiometry of the E_1W_6 heteroheptamers, the proteins were isolated and heated to dissociate the subunits and then further analyzed by a second analytical round of 10% SDS PAGE (Figure 2B). The relative intensity of E10 to W subunit was approximately 1:6 [$1:(5.8 \pm 0.5)$, $n = 3$]. For the $E5_1W_6$ and $E20_1W_6$ proteins, the relative intensity of E subunit to W subunit was also 1:6 [$E5_1W_6$, $1:(6.3 \pm 0.8)$, $n = 3$; $E20_1W_6$, $1:(6.5 \pm 0.7)$, $n = 3$]. The $E10_1W_6$ and $E20_1W_6$ samples were exposed for 20 days to obtain satisfactory signals, whereas the $E5_1W_6$ samples were exposed for 16 h.

Electrical Currents through Individual ELP Loop-Containing α HL Pores at Room Temperature. $E5_1W_6$, $E10_1W_6$, and $E20_1W_6$ were further examined by single-channel electrical recordings at room temperature (23 ± 0.5 °C). Currents flowing through individual α HL pores were recorded at +80 mV in 2 M KCl and 10 mM potassium phosphate buffer at pH 7.4. The current flowing through a wild-type α HL pore (W_7) was 164 ± 6 pA (e.g., the open-state current amplitude, $n = 7$ experiments, Figure 3A). Under these conditions, the

open state was of long duration (\sim hours).^{18,33} The W_7 pore remained opened for an indefinite period of time even at elevated temperatures, as also observed recently.³⁴ The open-state current amplitude through individual ELP loop-containing α HL pores was significantly reduced and decorated by transient current blockades, the nature of which depended on the ELP length (Table 1, Figure 3B–D) and temperature (see below).

For the engineered α HL pore with a short ELP [$E5_1W_6$, molecular mass (ELP) = 2.6 kDa, 36 amino acids, Table 1], we observed an open-state current amplitude of 139 ± 8 pA ($n = 4$), which is a reduction of $15\% \pm 2.5\%$ compared to the open state of the W_7 pore (Figure 3B). The very short-lived negative spikes (Figure 3B) are characterized by a mean duration, current amplitude, and frequency of 108 ± 12 μ s ($n = 4$), 98 ± 11 pA (70.5% of the open-state current amplitude, $n = 4$), and 140 ± 9 s⁻¹ ($n = 4$), respectively (Table 1).

For the engineered α HL pore with a medium-sized ELP

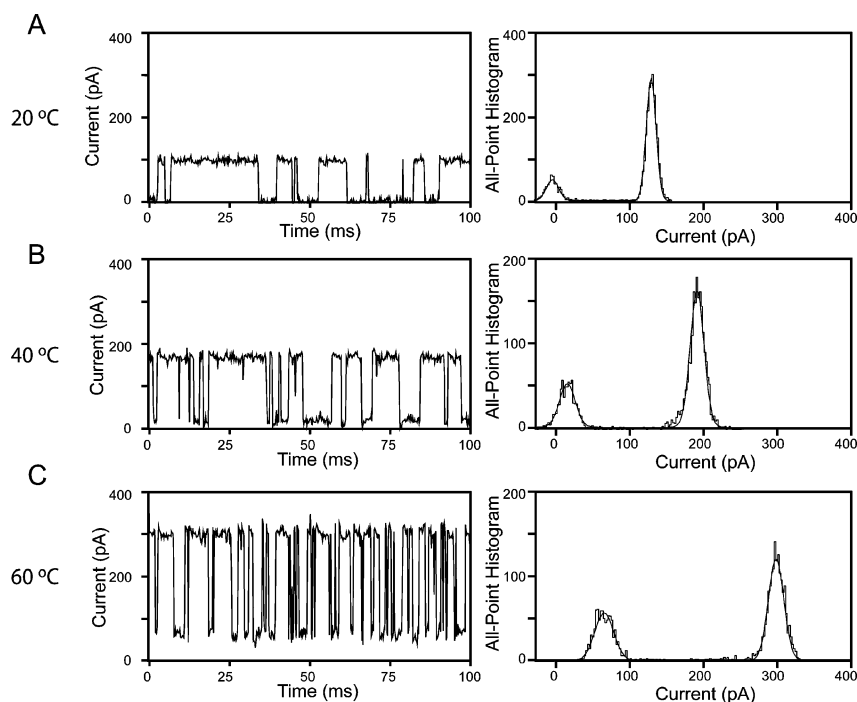
(33) Korchev, Y. E.; Bashford, C. L.; Alder, G. M.; Kasianowicz, J. J.; Pasternak, C. A. *J. Membr. Biol.* **1995**, *147*, 233–239.

(34) Kang, X. F.; Gu, L. Q.; Cheley, S.; Bayley, H. *Angew. Chem., Int. Ed.* **2005**, *44*, 1495–1499.

Table 1. Electrical Signatures of α HL Protein Pores with Single Polymers Attached within the Cavity at Room Temperature^a

modified pore	no. of amino acids	molecular mass (kDa)	$\Delta I/I_{WT}^b$	I/I_0^c	event frequency (s ⁻¹)	event duration (μ s)
α HL-PEG-3 kDa ^d	N/A	3.0	0.14 \pm 0.02 (5)	0.45 \pm 0.04 (5)	26 \pm 10 (5)	132 \pm 10 (5)
α HL-PEG-5 kDa ^e	N/A	5.0	0.18 \pm 0.03 (8)	0.42 \pm 0.03 (8)	0.20 \pm 0.02 (8)	13 700 \pm 2200 (8)
L65 ₁ W ₆ ^f	65	4.7	0.12 \pm 0.02 (3)	0.14 \pm 0.03 (3)	155 \pm 12 (3)	65 \pm 7 (3)
E5 ₁ W ₆ ^f	36	2.6	0.15 \pm 0.03 (4)	0.29 \pm 0.4 (4)	140 \pm 9 (4)	108 \pm 12 (4)
E10 ₁ W ₆ ^f	61	4.4	0.27 \pm 0.04 (14)	0.04 \pm 0.02 (14)	61 \pm 7 (14)	2600 \pm 280 (14)
E20 ₁ W ₆ ^f	111	8.1	0.39 \pm 0.5 (3)	0.01 \pm 0.01 (3)	16.0 \pm 2.7 (3)	45 000 \pm 5300 (3)

^a Values are means \pm SD for at least three separate single-channel experiments. Room temperature was 23 \pm 0.5 $^{\circ}$ C. ^b $\Delta I/I_{WT} = (I_{WT} - I_0)/I_{WT}$ is the reduction in single-channel current amplitude, brought about by the anchored polymer, and normalized to the value of the open state of the wild-type α HL pore (W₇). I_{WT} and I_0 are the open-state current amplitudes of the W₇ pore and the polymer-containing α HL pore, respectively. ^c I/I_0 is the residual current associated with polymer-induced current blockades, and normalized to the open-state current amplitude. ^d Values from Movileanu et al.²⁵ ^e Values from Howorka et al.³⁸ ^f Values from this work.

**Figure 4.** Temperature dependence of the single-channel current through the temperature-responsive pore E₁₀W₆ recorded at (A) 20, (B) 40, and (C) 60 $^{\circ}$ C. The transmembrane potential was +80 mV. The other experimental conditions were the same as those presented in Figure 3.

[E₁₀W₆, molecular mass (ELP) = 4.4 kDa, 61 amino acids, Table 1, Figure 3C], the open-state current amplitude is further reduced to 123 \pm 5 pA (n = 14). This result is consistent with the increase in ELP molecular mass, since a longer polymer is expected to produce a greater obstruction in the ionic flux through the α HL pore. The transient current blockades were also augmented (117 \pm 4 pA, 95% \pm 2% of the open-state current amplitude, n = 14), less frequent (61 \pm 7 s⁻¹, n = 14) and long-lived (2.6 \pm 0.28 ms, n = 14) (Table 1, Figure 3C).

In the case of a long ELP [E₂₀W₆, molecular mass (ELP) = 8.1 kDa, 111 amino acids, Table 1, Figure 3D], we found a substantial reduction in the open-state current amplitude to 104 \pm 5 pA (n = 3). The transient full current blockades (102 \pm 5 pA, 99% \pm 1% of open-state current amplitude, n = 3) were very long-lived (45.0 \pm 5.3 ms, n = 3) and much less frequent (16 \pm 2.7 s⁻¹, n = 3) (Table 1, Figure 3D).

Temperature Dependence of an ELP Loop-Containing α HL Protein Pore. The E₅W₆ pore [molecular mass (ELP) = 2.7 kDa, Table 1] produced short-lived transient spikes at room temperature, with an average duration of 108 \pm 12 μ s (n = 4), but they were hardly resolvable at elevated temperatures (data not shown). In contrast, the very long-lived current blockades observed with the E₂₀W₆ pore were presumably

caused by small available volume per ELP length. The E₁₀W₆ pore showed full current blockade events of millisecond time-scale duration at 20 $^{\circ}$ C (Figure 4A), and they were resolvable throughout the temperature range examined in this work (20–60 $^{\circ}$ C). Therefore, the temperature dependence of the features of the E₁₀W₆ pore was further examined.

The open-state current amplitude and individual current blockades of E₁₀W₆ were highly temperature-sensitive (Figure 4). For example, the open-state current amplitude of the ELP loop-containing α HL pore increased with the temperature, from 119 \pm 7 pA (n = 8) at 20 $^{\circ}$ C to 203 \pm 11 pA (n = 5) at 40 $^{\circ}$ C and 291 \pm 12 pA (n = 5) at 60 $^{\circ}$ C (Figure 4). This finding was consistent with the change in the conductivity of the buffer solution (2 M KCl and 10 mM potassium phosphate, pH 7.4) from 179 mS/cm at 20 $^{\circ}$ C to 240 mS/cm at 40 $^{\circ}$ C and 302 mS/cm at 60 $^{\circ}$ C (Supporting Information, Figure S2). Using the log likelihood ratio (LLR) test,^{18,35} we found two types of blockades with the same temperature-dependent current amplitude but with distinct temperature-dependent durations and probabilities. For example, at 20 $^{\circ}$ C, we observed full transient current blockades with two durations: $\tau_{\text{off-1}} = 390 \pm 36 \mu$ s,

(35) McManus, O. B.; Magleby, K. L. *J. Physiol. (London)* **1988**, *402*, 79–120.

Table 2. Temperature Dependence of Single-Channel Transient Current Blockade Events Analyzed for the E10₁W₆ Pore^a

temp (°C)	P_1^b	P_2^b	τ_{on}^c (ms)	τ_{off-1}^d (μ s)	τ_{off-2}^d (ms)	τ_{off}^e (ms)
20	0.05 ± 0.02	0.95 ± 0.02	19 ± 1.7	390 ± 36	4.2 ± 0.24	4.0 ± 0.38
25	0.09 ± 0.02	0.91 ± 0.02	14 ± 1.8	310 ± 42	2.8 ± 0.18	2.6 ± 0.28
30	0.42 ± 0.03	0.58 ± 0.03	9.7 ± 1.1	291 ± 32	2.6 ± 0.21	1.6 ± 0.19
35	0.52 ± 0.03	0.48 ± 0.03	7.5 ± 1.5	240 ± 25	2.3 ± 0.19	1.2 ± 0.11
40	0.67 ± 0.03	0.33 ± 0.03	5.2 ± 0.9	231 ± 27	1.8 ± 0.16	0.75 ± 0.091
45	0.77 ± 0.03	0.23 ± 0.03	4.0 ± 0.6	162 ± 19	1.4 ± 0.13	0.44 ± 0.076
50	0.83 ± 0.02	0.17 ± 0.02	3.2 ± 0.7	156 ± 18	1.2 ± 0.14	0.32 ± 0.063
55	0.89 ± 0.03	0.11 ± 0.03	2.4 ± 0.5	135 ± 15	0.89 ± 0.12	0.22 ± 0.018
60	0.95 ± 0.02	0.05 ± 0.02	1.9 ± 0.4	120 ± 16	0.72 ± 0.083	0.15 ± 0.021

^a The values are means ± SD for at least five different single-channel experiments. ^b P_1 and P_2 are the probabilities of the short- and long-lived substates, respectively. ^c τ_{on} , the mean duration of interevent intervals, was determined directly from the “on” dwell-time histograms. $\tau_{on-1} = \tau_{on}/P_1$ and $\tau_{on-2} = \tau_{on}/P_2$, with $P_1 + P_2 = 1$.¹⁸ ^d At a confidence level of 0.95, the best model for a dwell-time histogram was a two-exponential fit. Fits to a three-exponential fit were not significantly better, as judged by the log likelihood ratio (LLR) value.^{18,35} τ_{off-1} and τ_{off-2} , the mean durations of the short- and long-lived states, respectively, were determined directly from the “off” dwell-time histograms. ^e τ_{off} , the overall mean duration of the transient current blockade events, was calculated from the formula $\tau_{off} = P_1\tau_{off-1} + P_2\tau_{off-2}$.

with a probability $P_1 = 0.05 \pm 0.02$ (the short-lived states), and $\tau_{off-2} = 4.20 \pm 0.24$ ms, with a probability $P_2 = 0.95 \pm 0.02$ (the long-lived states) ($n = 8$, Table 2). The mean durations of the short- and long-lived states were temperature-sensitive. At 40 °C, the mean duration of the short-lived states was $\tau_{off-1} = 231 \pm 27 \mu$ s ($P_1 = 0.67 \pm 0.03$, $n = 5$), whereas the mean duration of the long-lived states was $\tau_{off-2} = 1.8 \pm 0.16$ ms ($P_2 = 0.33 \pm 0.03$, $n = 5$) (Table 2). At 60 °C, the mean duration of the short-lived states was $\tau_{off-1} = 120 \pm 16 \mu$ s ($P_1 = 0.95 \pm 0.02$, $n = 5$), whereas the mean duration of the long-lived states was $\tau_{off-2} = 720 \pm 83 \mu$ s ($P_2 = 0.05 \pm 0.02$, $n = 5$) (Table 2). The total event frequency increased substantially with the temperature from 53.0 ± 5.7 s⁻¹ at 20 °C to 185 ± 17 s⁻¹ at 40 °C and 495 ± 38 s⁻¹ at 60 °C.

Temperature Dependence of a Gly/Ser-Based Peptide-Containing α HL Protein Pore. We examined whether the single-channel electrical signature of the peptide loop-containing α HL pores is dependent on the sequence of the exogenous peptide. We carried out single-channel recordings with a Gly/Ser-based peptide loop-containing α HL pore, L65₁W₆, under conditions similar to those used for the E10₁W₆ pore. The Gly/Ser-rich peptide, which has the sequence GGG-(SGSGSGSSG)₆SG, is similar in length (~ 65 residues) to the ELP peptide from the E10₁W₆ pore (61 amino acids). At room temperature, in contrast to the data recorded for the E10₁W₆ pore, the single-channel electrical recordings of the L65₁W₆ pore revealed very short-lived ($55 \pm 7 \mu$ s, $n = 3$), but highly frequent (155 ± 12 s⁻¹) current spikes (Figure 5). At 20 °C, the open-state current amplitude of the L65₁W₆ pore was 135 ± 7 pA ($n = 3$), whereas the maximum amplitude of the transient current blockades was 118 ± 10 pA ($n = 3$) (Figure 5). At 60 °C, these amplitudes were 312 ± 12 pA ($n = 3$) and 268 ± 12 pA ($n = 3$), respectively. The values of the spike amplitudes were not significantly affected by the rise time of the filter ($\sim 15 \mu$ s).^{36,37}

Discussion

Features of the ELP Loop-Containing α HL Pores. The engineered α HL pore with a short ELP loop [molecular mass (ELP) ~ 2.6 kDa] showed short-lived and highly frequent current blockades (Figure 3B, Table 1). We found similar results with a highly flexible poly(ethylene glycol) (PEG-3 kDa) chain covalently attached to the central part of the cavity at position

106 (Table 1).^{25,38} On the basis of this previous work, we interpret the short-lived negative spikes as excursions of the ELP loop into the β -barrel part of the α HL pore. In the case of experiments with the PEG-modified α HL pores, this interpretation has been bolstered by observations made with the untethered end of the polymer locked at either side of the membrane.²⁵ The amplitude of the PEG-induced spikes was similar to the value of the permanent current blockade when the untethered end of PEG was locked at the trans side of the bilayer. The short-lived spikes produced by the short ELP loop suggested a high mobility of the polypeptide within the cavity (~ 39 500 Å³). In contrast, the millisecond time-scale current blockades obtained with the E10₁W₆ pore were consistent with a less flexible ELP loop.

The very long ELP loop from the E20₁W₆ pore was strikingly less mobile than those from the E5₁W₆ and E10₁W₆ pores, as judged by long-lived, large-amplitude, and infrequent current blockades. The high entropic cost for the excursions of the ELP loop into the β barrel is also suggested by a substantially increased amplitude of the noise for the closed states, most likely because of the strong interactions between the polypeptide and the pore walls (Figure 3D). The dwell-time histograms of the ELP loop-induced transient current blockades were fitted by a two-exponential distribution (Table 2). One possible explanation is that the ELP loop partitions into the β -barrel constriction in different conformations. Interestingly, we noticed that the ELP loop-induced current blockades have uniform amplitude. A uniform amplitude has also been observed for the transient current blockades produced by PEGs when permanently anchored within the cavity of the α HL pore.^{25,38}

The engineered α HL pores containing peptide loops similar in length, but different in sequence, exhibited various single-channel electrical signatures. The E10-induced events were large-amplitude current blockades of millisecond time-scale duration. In contrast, the experiments with the L65₁W₆ pore [molecular mass (loop) = 4.7 kDa, Table 1] showed very short-lived and highly frequent current blockades (Figure 5), which is in accord with increased flexibility of the Gly/Ser-based peptide loop because of the absence of bulky side chains at Gly residues.

Comparison of the ELP Loop-Containing α HL Pores with PEG-Modified α HL Pores. It is instructive to compare the single-channel electrical signature of the ELP loop-containing

(36) McManus, O. B.; Blatz, A. L.; Magleby, K. L. *Pflugers Arch.* **1987**, *410*, 530–553.

(37) Colquhoun, D.; Sigworth, F. J. *Fitting and statistical analysis of single-channel records*. In *Single-channel recording*; Sackmann, B. N. E., Ed.; Plenum Press: New York, 1995; pp 483–587.

(38) Howorka, S.; Movileanu, L.; Lu, X. F.; Magnon, M.; Cheley, S.; Braha, O.; Bayley, H. *J. Am. Chem. Soc.* **2000**, *122*, 2411–2416.

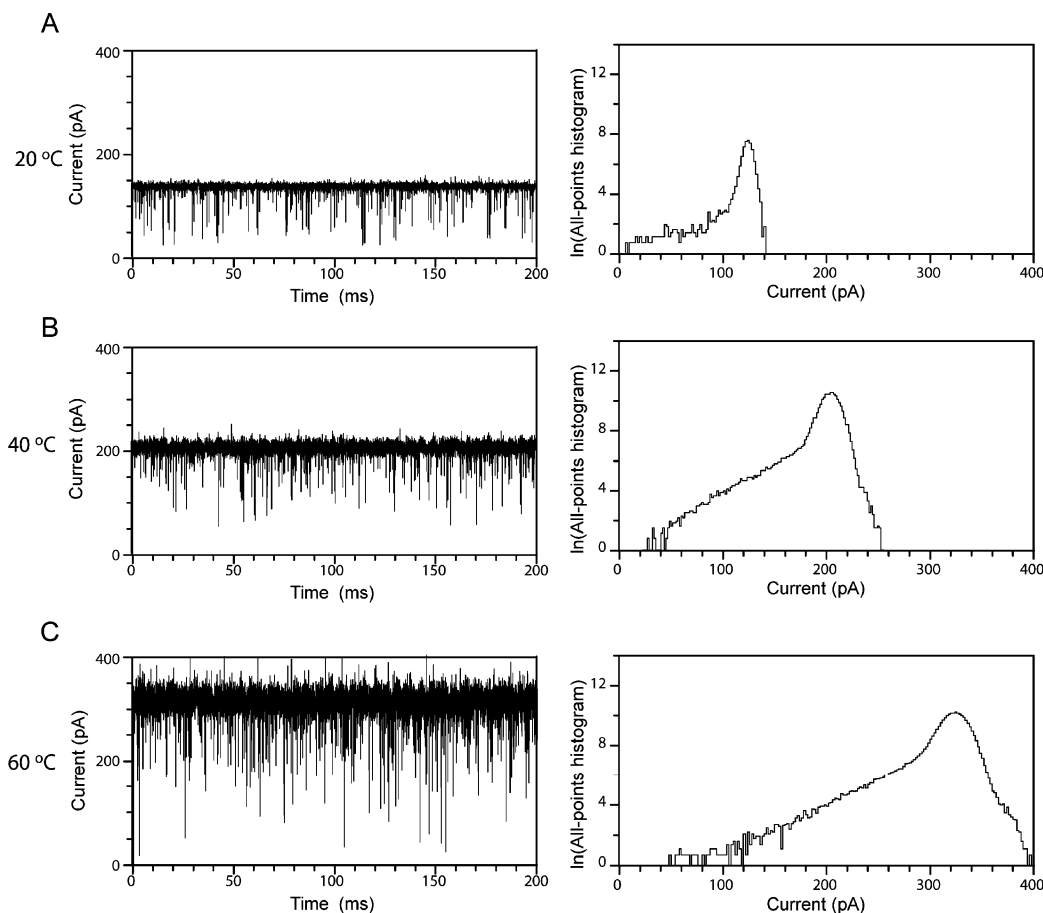


Figure 5. Temperature dependence of the single-channel current through the L651W₆ pore, which contains a Gly/Ser-based loop, recorded at (A) 20, (B) 40, and (C) 60 °C. The transmembrane potential was +80 mV. The other conditions were the same as those presented in Figure 3.

α HL pores with those of the PEG-modified α HL pores, which feature a single poly(ethylene glycol) (PEG) anchored within the cavity of the lumen (Table 1).^{25,38} In both cases, an increment in molecular mass of about 2 kDa (i.e., α HL-PEG-3 kDa to α HL-PEG-5 kDa or E5₁W₆ to E10₁W₆, Table 1) enhanced the duration of transient current blockades from about 100 μ s to several milliseconds, suggesting that the long polymers [PEG-5 kDa and (VPGGG)₁₀] are less mobile than the short ones [PEG-3 kDa and (VPGGG)₅, respectively]. The frequency of the transient current blockades decreased substantially in the case of the PEG-modified α HL pores (α HL-PEG-3 kDa to α HL-PEG-5 kDa, a decrease of 2 orders of magnitude; Table 1), whereas little change in frequency was found for the ELP loop-containing α HL pores (E5₁W₆ to E10₁W₆, a decrease of $\sim 57\%$; Table 1). At room temperature, the amplitude of the transient current blockades made by ELPs was significantly greater than that made by PEGs with similar molecular mass [i.e., (VPGGG)₅ versus PEG-3 kDa and (VPGGG)₁₀ versus PEG-5 kDa, Table 1]. For example, at room temperature, a medium-sized ELP loop [molecular mass (ELP) ~ 4.4 kDa] produced a current blockade of $96\% \pm 2\%$ of a full open state, whereas the PEG-5 kDa produced a current blockade of $58\% \pm 3\%$ of a full open state (Table 1). These dissimilarities between the features of the ELP loop-containing α HL pores and PEG-modified α HL pores are determined by differences in the local flexibility of the anchored polymers. Also, the PEG chain has a single point of attachment,^{25,38} while the ELP loop does not have a free end.¹⁷

Recently, Kong and Muthukumar³⁹ have performed Langevin dynamics and Poisson–Nernst–Planck (PNP) calculations to simulate the current fluctuations caused by a single PEG covalently anchored within the α HL cavity.²⁵ The PNP calculations confirmed that the short-lived and large-amplitude negative spikes are due to the obstruction of the β barrel by the tethered PEG. A detailed mechanistic understanding of the transient current blockades produced by the ELP loop might be addressed by using a similar computational methodology.^{39,40} These simulations, for example, might explain why the amplitudes of the transient current blockades are uniform or to what extent the ELP loop partitions into the β -barrel domain of the α HL pore. An interesting question to be addressed is whether the two categories of transient current blockades are caused by ELP partitioning into the barrel while in different conformations or by the interaction of the ELP loop with different binding sites. Understanding this mechanistic problem would certainly ease the interpretation of the values of thermodynamic and kinetic parameters, such as entropies and enthalpies that can be derived from Arrhenius–van’t Hoff-type temperature-dependence plots^{14,41,42} of the rate constants of association (k_{on}) and dissociation (k_{off}). We plan to carry out such a detailed

(39) Kong, C. Y.; Muthukumar, M. *J. Am. Chem. Soc.* **2005**, *127*, 18252–18261.

(40) Muthukumar, M.; Kong, C. Y. *Proc. Natl. Acad. Sci. U.S.A.* **2006**, *103*, 5273–5278.

(41) Manno, M.; Emanuele, A.; Martorana, V.; San Biagio, P. L.; Bulone, D.; Palma-Vittorelli, M. B.; McPherson, D. T.; Xu, J.; Parker, T. M.; Urry, D. W. *Biopolymers* **2001**, *59*, 51–64.

(42) Howorka, S.; Movileanu, L.; Braha, O.; Bayley, H. *Proc. Natl. Acad. Sci. U.S.A.* **2001**, *98*, 12996–13001.

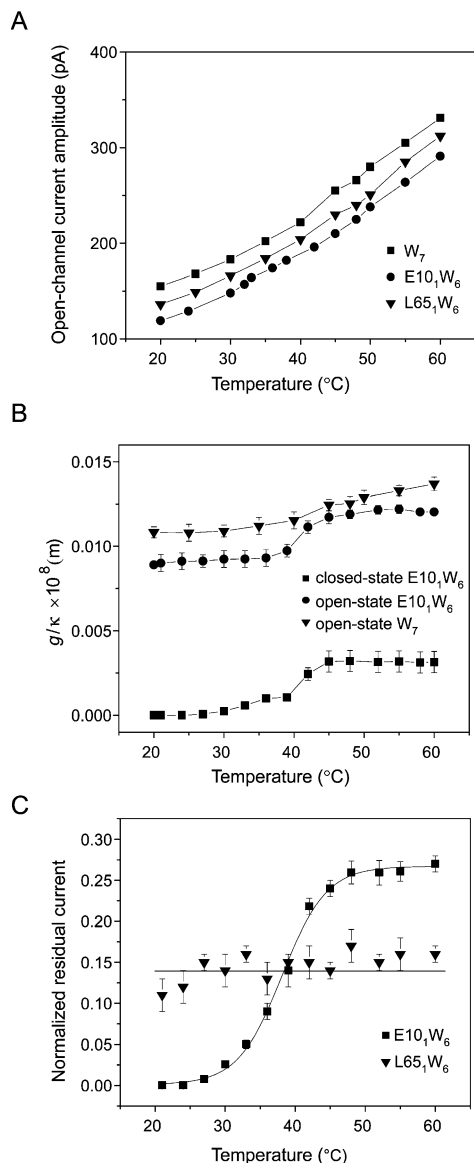


Figure 6. Temperature dependence of the single-channel conductance of the peptide loop-containing α HL pore: (A) Temperature dependence of the open-state current amplitude of the pores W_7 , $L65_1W_6$, and $E10_1W_6$. (B) Ratio between single-channel conductance and solution conductivity for open-state W_7 and open- and closed-state $E10_1W_6$ pores at various temperatures. (C) Temperature dependence of the residual current in the closed state normalized to the value corresponding to the open-state current amplitude for $L65_1W_6$ and $E10_1W_6$ pores. For the $E10_1W_6$ pore, the values of open and closed states were derived from all-points amplitude histograms (Figure 4, right-hand panels). For the $L65_1W_6$ pore, the value of the residual current was deduced from the maximum current blockade induced by the Gly/Ser-based peptide loop. The transmembrane potential was +80 mV.

thermodynamic and kinetic analysis combined with a computational approach in a future publication.

Temperature Dependence of the Single-Channel Conductance of the ELP Loop-Containing α HL Pore. The temperature dependence of the open-state current amplitudes of the W_7 , $L65_1W_6$, and $E10_1W_6$ pores is shown in Figure 6A. The open-state currents of the W_7 pore are consistent with those measured recently in 1 M KCl solution.³⁴ The values of the open-state currents for the $E10_1W_6$ and $L65_1W_6$ pores were smaller than that of the W_7 pore, which is in accordance with a decreased ionic flux through a pore with a polymer-filled cavity. The open-state current amplitude of the W_7 , $L65_1W_6$,

and $E10_1W_6$ pores did not increase linearly with temperature. In contrast, we found a linear dependence of the conductivity of the electrolyte solution with the temperature (Supporting Information, Figure S2). Therefore, we normalized the single-channel conductance values associated with the open and peptide loop-induced blocked states to the conductivity of the bulk solution over the temperature range 20–60 $^{\circ}\text{C}$ (Figure 6B). Strikingly, the normalized conductance for the open and ELP-induced blocked states showed a two-state profile with the midpoints located at 40.0 ± 0.4 and 42.2 ± 0.4 $^{\circ}\text{C}$ ($n = 5$, Figure 6B).

We also normalized the residual current (I_r) associated with the ELP-induced current blockades to the value of the open-state current amplitude (I_0) of the ELP loop-containing α HL pores. For the $E10_1W_6$ pores, this value increased gradually from 0 (i.e., full current blockades) at 20 $^{\circ}\text{C}$ to a maximum value of 0.27 ± 0.02 at 60 $^{\circ}\text{C}$ (i.e., partial current blockades) (Figure 6C). The normalized residual current (I_r/I_0) showed a temperature-dependent two-state profile, with the midpoint located at 38.1 ± 0.4 $^{\circ}\text{C}$ ($n = 5$, Figure 6C). We interpret this result as a temperature-induced hydrophobic collapse of the anchored ELP. Spectroscopic,^{9,12–14,41,43} thermodynamic,^{5,12,44} and atomic force microscopic measurements^{10,11,45} and molecular dynamics simulations^{15,20–22,46} have established that an ELP behaves as a two-state system that undergoes an *inverse temperature* folding transition. We conclude that below its transition temperature, T_t , the ELP loop is in expanded conformation^{7,8,10,20,21} and produces full current blockades. Above T_t , the ELP loop is dehydrated due to hydrophobic collapse,^{7–15,20–22} producing partial current blockades.

Because the thermal properties of ELP are dependent on the peptide features (e.g., the sequence of the repeat unit, its length) and the environment (e.g., salt concentration, pH, temperature), we examined the transition temperature of the mid-sized ELP [(VPGGG)₁₀Y-NH₂] by light scattering assay and CD spectroscopy. A solution of 100 μM (VPGGG)₁₀Y-NH₂ in 2 M KCl and 10 mM potassium phosphate buffer, pH 7.4, showed temperature transitions with midpoints at 39.6 $^{\circ}\text{C} \pm 0.2$ ($n = 3$) and 38.4 $^{\circ}\text{C} \pm 0.26$ ($n = 5$), according to a light scattering assay (350 nm) and CD spectroscopy (molar ellipticity at 222 nm), respectively (Supporting information, Figure S3). The (VPGGG)_{*n*}-based ELPs exhibit a transition temperature of ~ 55 $^{\circ}\text{C}$ in phosphate-buffered saline solution.⁶ According to previous studies in Urry's group,⁵ the salt concentration decreases T_t by 14 $^{\circ}\text{C}/[\text{c}]$, where $[\text{c}]$ is the molar NaCl concentration. If we assume that NaCl and KCl have similar effects on the transition temperatures of ELPs, the estimated T_t of (VPGGG)_{*n*} in 2 M KCl and 10 mM phosphate buffer, pH 7.4, would be about 27 $^{\circ}\text{C}$. Recently, Meyer and Chilkoti have shown that T_t increases by decreasing the ELP molecular mass.⁴⁷ Since the molecular mass of the ELP loop used in this study is much smaller than that in Urry's work,^{5,6} we qualitatively conclude that the inverse transition temperature of the VPGGG-based ELPs should be

(43) Zhang, Y.; Trabbic-Carlson, K.; Albertorio, F.; Chilkoti, A.; Cremer, P. S. *Biomacromolecules* **2006**, *7*, 2192–2199.

(44) Samouillan, V.; Andre, C.; Dandurand, J.; Lacabanne, C. *Biomacromolecules* **2004**, *5*, 958–964.

(45) Yang, G.; Woodhouse, K. A.; Yip, C. M. *J. Am. Chem. Soc.* **2002**, *124*, 10648–10649.

(46) Li, B.; Alonso, D. O. V.; Bennion, B. J.; Daggett, V. *J. Am. Chem. Soc.* **2001**, *123*, 11991–11998.

(47) Meyer, D. E.; Chilkoti, A. *Biomacromolecules* **2002**, *3*, 357–367.

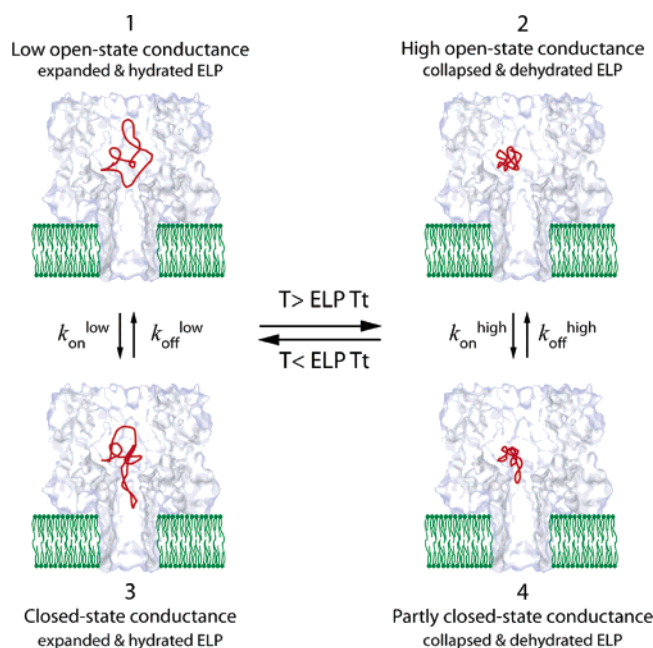


Figure 7. Model for the temperature-dependent transient current blockades of the E10₁W₆ pore probed by single-channel recording in planar lipid bilayers.

greater than 27 °C, which is in accord with our bulk measurements (Supporting Information, Figure S3).

A simplified kinetic model with four states, which is based on the observed temperature-induced changes in the open- and closed-state current amplitudes of the E10₁W₆ pore, is presented in Figure 7. The ELP loop undergoes a reversible folding temperature transition at ~40 °C. States 1 and 3 represent the open and closed states, respectively, of the ELP loop-containing α HL pore at temperatures below T_t . In these states, the peptide is fully hydrated and expanded. States 2 and 4 indicate the open and partly closed states, respectively, at temperatures above T_t . In these states, the ELP loop is dehydrated, and its structure is collapsed. The excursions of a low-temperature expanded ELP into the β -barrel part of the pore produce a full current blockade (state 3). In contrast, the excursions of a high-temperature collapsed ELP produce a partial current blockade (state 4).

Conclusions. In previous studies from other groups, stimulus-responsive polymers have been attached to proteins to modulate ligand-binding² and enzymatic activities⁴⁸ and to produce temperature-induced transitions in protein-based hydrogels.⁴⁹ In the present work, we have used genetic engineering to place a temperature-responsive gating mechanism within the cavity of the lumen of the α HL pore. The ELP loop-containing α HL pore is stable in SDS–polyacrylamide gels and functional, as judged by its pore-forming ability.

Engineered α HL pores, with functional polymers placed within the cavity, have been already developed.^{25,32,38,42,50} There

is no fundamental technical problem that would prevent replacing an ELP by other functional polypeptide loops that respond to external physical or chemical stimuli, including pH, divalent metal ions, light, ionic strength, or chemical denaturants. The design of channels and pores with stimulus-activated gating mechanisms is a potentially fertile area.^{51,52} Recently, a light-activated nanovalve has been engineered by the attachment of synthetic photosensitive compounds to a mechanosensitive channel (MscL).⁵³ Kramer and colleagues⁵⁴ have also designed a light-responsive K⁺ ion channel. The gating mechanism consists of a pore blocker and a photoisomerizable azobenzene. The azobenzene assumes a trans configuration in long-wavelength light, enabling the blocker to reach the pore. In contrast, the azobenzene assumes a cis configuration in short-wavelength light. In the latter case, the blocker cannot reach the pore, thus allowing ion conduction.

Finally, knowing the relationships between structure and the functional characteristics of temperature-responsive peptides confined in nanocavities may contribute significantly to the rational design of “intelligent” biomaterials. For example, ELP sequences within α HL pores might be engineered further to enable the temperature-controlled release of drugs from lipid vesicles or the permeabilization of mammalian cells for the introduction of cryoprotectants.^{55,56}

Acknowledgment. The experimental part of this paper was done at Texas A&M University System Health Science Center. We thank Jim Abbott (Dagan Corp.) for help concerning a customized noise-free thermal stage for bilayer recordings, Steve Cheley (Texas A&M University) for the pT7- α HL-D4 plasmid, and Aaron Wolfe for the values of the conductivity of KCl solutions at various temperatures. This work was supported by grants from the National Institutes of Health, the Office of Naval Research, and the Medical Research Council. H.B. is the holder of a Royal Society–Wolfson Research Merit Award. L.M. thanks Syracuse University for start-up funds.

Supporting Information Available: Detailed diagrams for the construction of the ELP-containing α HL genes, temperature dependence of the conductivity of the buffer solution, and transition temperature of (VPGGG)₁₀Y-NH₂ in 2 M KCl. This material is available free of charge via the Internet at <http://pubs.acs.org>.

JA065827T

(48) Shimoboji, T.; Larenas, E.; Fowler, T.; Kulkarni, S.; Hoffman, A. S.; Stayton, P. S. *Proc. Natl. Acad. Sci. U.S.A.* **2002**, *99*, 16592–16596.

(49) Wang, C.; Stewart, R. J.; Kopecek, J. *Nature* **1999**, *397*, 417–420.

(50) Bayley, H.; Cremer, P. S. *Nature* **2001**, *413*, 226–230.

(51) Bayley, H. *Curr. Opin. Biotechnol.* **1999**, *10*, 94–103.

(52) Bayley, H.; Braha, O.; Cheley, S.; Gu, L. Q. Engineered nanopores. In *NanoBiotechnology*; Niemeyer, C. M. a. M. C. A., Ed.; Wiley-VCH: Weinheim, Germany, 2004; pp. 93–112.

(53) Kocer, A.; Walko, M.; Meijberg, W.; Feringa, B. L. *Science* **2005**, *309*, 755–758.

(54) Banghart, M.; Borges, K.; Isacoff, E.; Trauner, D.; Kramer, R. H. *Nat. Neurosci.* **2004**, *7*, 1381–1386.

(55) Eroglu, A.; Russo, M. J.; Bieganski, R.; Fowler, A.; Cheley, S.; Bayley, H.; Toner, M. *Nat. Biotechnol.* **2000**, *18*, 163–167.

(56) Chen, T.; Acker, J. P.; Eroglu, A.; Cheley, S.; Bayley, H.; Fowler, A.; Toner, M. *Cryobiology* **2001**, *43*, 168–181.